IEEE Access
Multidisciplinary | Rapid Review | Open Access Journal

Received December 10, 2018, accepted January 2, 2019, date of publication February 1, 2019, date of current version February 12, 2019.

Digital Object Identifier 10.1109/ACCESS.2019.2893112

Eight-Element Dual-Polarized MIMO Slot Antenna System for 5G Smartphone Applications

NASER OJAROUDI PARCHIN[1], YASIR ISMAEL ABDULRAHEEM AL-YASIR[1], AMMAR H. ALI[1], ISSA ELFERGANI[2], (Member, IEEE), JAMES M. NORAS[1], JONATHAN RODRIGUEZ[2,3], (Senior Member, IEEE), AND RAED A. ABD-ALHAMEED[1], (Senior Member, IEEE)

[1]Faculty of Engineering and Informatics, University of Bradford, Bradford BD7 1DP, U.K.
[2]Instituto de Telecomunicações, Campus Universitário de Santiago, 3810-193, Aveiro, Portugal
[3]Mobile and Satellite Communications Research Group, University of South Wales, Treforest CF37 1DL, U.K.

Corresponding author: Naser Ojaroudi Parchin (n.ojaroudiparchin@bradford.ac.uk)

This project has received funding from the European Union's Horizon 2020 research and innovation programme under grant agreement H2020-MSCA-ITN-2016 SECRET-722424.

ABSTRACT In this paper, we propose an eight-port/four-resonator slot antenna array with a dual-polarized function for multiple-input-multiple-output (MIMO) 5G mobile terminals. The design is composed of four dual-polarized square-ring slot radiators fed by pairs of microstrip-line structures. The radiation elements are designed to operate at 3.6 GHz and are located on the corners of the smartphone PCB. The square-ring slot radiators provide good dual-polarization characteristic with similar performances in terms of fundamental radiation characteristics. In order to improve the isolation and also reduce the mutual coupling characteristic between the adjunct microstrip-line feeding ports of the dual-polarized radiators, a pair of circular-ring/open-ended parasitic structures is embedded across each square-ring slot radiator. The −10-dB impedance bandwidth of each antenna-element is 3.4–3.8 GHz. However, for −6-dB impedance bandwidth, this value is 600 MHz (3.3–3.9 GHz). The proposed MIMO antenna offers good S-parameters, high-gain radiation patterns, and sufficient total efficiencies, even though it is arranged on a high-loss FR-4 dielectric. The SAR function and the radiation characteristics of the proposed design in the vicinity of user-hand/user-head are studied. A prototype of the proposed smartphone antenna is fabricated, and good measurements are provided. The antenna provides good features with a potential application for use in the 5G mobile terminals.

INDEX TERMS 5G, dual-polarized antenna, MIMO system, mobile terminal, ring slot antenna.

I. INTRODUCTION

MIMO wireless technology can highly improve the data rate, capacity, and link reliability of wireless systems through multi-path data transmission and reception. MIMO system is currently employed in 4G user equipment and is a promising technology for use in the future 5G mobile terminals [1], [2]. One of the promising frequency bands for sub-6-GHz MIMO 5G communications is 3.4-3.8 GHz which has been proposed by Ofcom, UK [3].

There are many requirements of antenna designing such as low-profile, ease of fabrication, and high-isolation which must be considered to design a qualified MIMO antenna system for smartphones [4]. Recently, several works were reported in the literature for 5G mobile terminals[5]–[10]. However, all these antennas either provide narrow impedance bandwidth or use multiple radiators with single-polarization at different sides of PCB which occupy a huge space or increase the complexity of the MIMO system. A multiple-antenna design for 5G smartphones applications is proposed in [11] which is only covering 3.5 to 3.7 of 5G bands and also the maximum mutual coupling of the antenna elements is −10 dB which could affect wireless system performance, antenna efficiency, as well as amplitude and phase of the radiators. Gap-coupled loop antenna array design with an impedance bandwidth of 3.4-3.8 GHz has been proposed in [12] for the future smartphone application. However, since the design is not planar, fabrication of this kind of antennas would be a challenging issue for the antenna engineers. In [13], an eight-port MIMO antenna with dual-polarized function has been proposed for 5G smartphone Applications. Its bandwidth is very narrow and not wide enough to cover more than 100 MHz. In addition, the radiators of the antenna

cannot cover both sides of the mobile-phone PCB, since they are patch antennas. Another design of dual-polarized MIMO antenna with narrow bandwidth and non-planar structure is proposed in [14]. Furthermore, the reduction of the mutual coupling between the closely-spaced radiators is not investigated in most of the recently published papers about 5G mobile terminals. Wide bandwidth, low mutual coupling, and compact size are some of the major characteristics concerned for designing a dual-polarized antenna [15]. We propose here a new design of a compact MIMO slot antenna system using four-radiator/eight-port dual-polarized antennas which provide wide bandwidth and improved isolation properties.

Slot antennas have become very attractive candidates for wireless systems owns lots of interesting features like simple structure, wide impedance bandwidth, good isolation, easy integration with active devices, and etc. Due to the fact that cutting a slot in the bottom layer of an antenna lets it radiates on both sides of the substrate, makes the slot antenna a good choice for designing the dual-polarized antenna to be used in wireless communication platforms [16]. Moreover, compared with the other conventional antennas (such as Dipole, Monopole, Yagi, and etc.) it is much easier to achieve the dual-polarized characteristic for the slot antenna with the microstrip-line feeding [17].

The configuration of the dual-polarized slot antenna element contains a compact square-ring slot antenna fed by rectangular microstrip-lines. In addition, a pair of circular-ring/open-ended parasitic structures has been employed across the ring slot to reduce the mutual coupling characteristic between two microstrip-line feeding ports. For the proposed 5G antenna, the ring-slot radiators are placed at four corners of the PCB to provide full radiation coverage with different polarizations. The single-element and the proposed antenna array exhibit good characteristics for MIMO applications. Their fundamental properties have been investigated in the following Sections. In addition, the radiation characteristics of the smartphone antenna array system in the presence of human hands/head have been studied and good results are achieved. Furthermore, the proposed MIMO antenna exhibits good SAR characteristic with low levels over the entire operation band that makes it suitable for use in the cellular applications.

II. DUAL-POLARIZED SINGLE-ELEMENT ANTENNA

In this section, the fundamental properties of the single element dual-polarized square-ring slot resonator with various design parameters have been studied and the simulation and measurement results are presented. Figure 1 illustrates a transparent view of the antenna configuration. As seen, the antenna configuration is composed of a square-ring slot in the ground plan with a pair of rectangular microstrip-lines employed at different top-side of the slot resonator. Furthermore, a pair of parasitic structures is used across the square-ring slot resonator on the top layer of the antenna. The antenna has a low profile of $W_S \times W_S$ and has been designed on an FR4 dielectric with relative permittivity 4.4, loss tangent

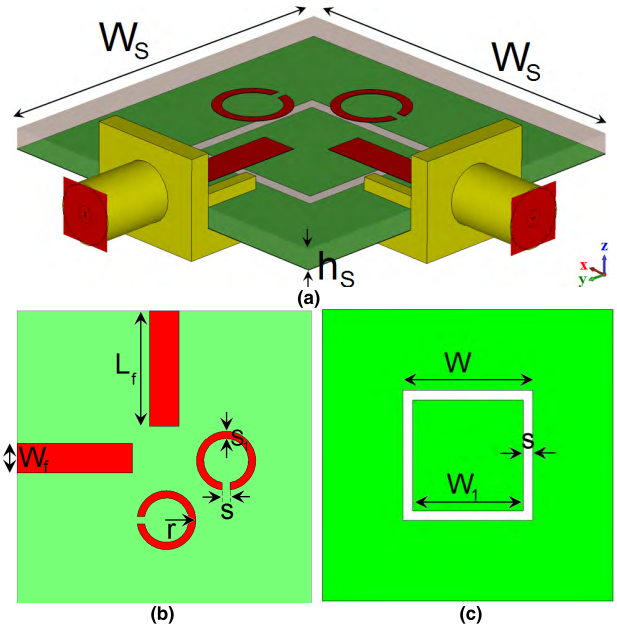

FIGURE 1. The proposed slot antenna configuration, (a) side-view, (b) top-layer, and (c) bottom-layer.

TABLE 1. The values of the design parameter.

Parameter	Value (mm)
W	13.4
h_S	1.6
W_f	3
L_f	11.75
W_S	30
W_1	11.9
W_2	13.15
S	0.75
S_1	0.75
L_1	9
d	5.95
r	3

0.025 and thickness 1.6 mm. The parameter values of the single-element antenna and also the proposed MIMO array are specified in Table 1.

Each port of the proposed slot antenna provides a linear-polarization. The polarization type (vertical or horizontal) of each port relates to the placement of the antenna in the RF system. The configurations of the various structures studied for designing the dual-polarized microstrip-fed slot antenna were displayed in Fig. 2. The simulated S-parameters for a conventional dual-polarized microstrip-fed square-ring slot antenna (Fig. 2(a)), the antenna with only one circular-ring/open-ended parasitic structure (Fig. 2(b)), and the proposed single-element dual-polarized slot antenna structure (Fig. 2(c)) are illustrated and compared in Fig. 3. As illustrated, by employing the proposed parasitic structures on the top layer of the FR-4 dielectric and across the slot radiator, the desired impedance bandwidth, covering the frequency range

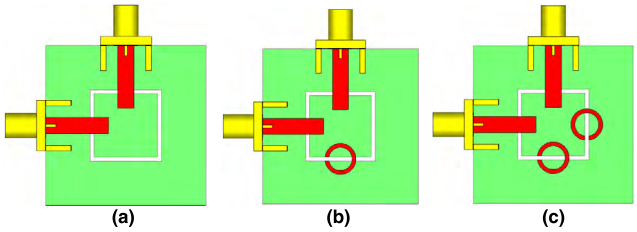

FIGURE 2. Ordinary square-ring dual-polarized antenna, (b) the antenna with a parasitic structure, and (c) the proposed design.

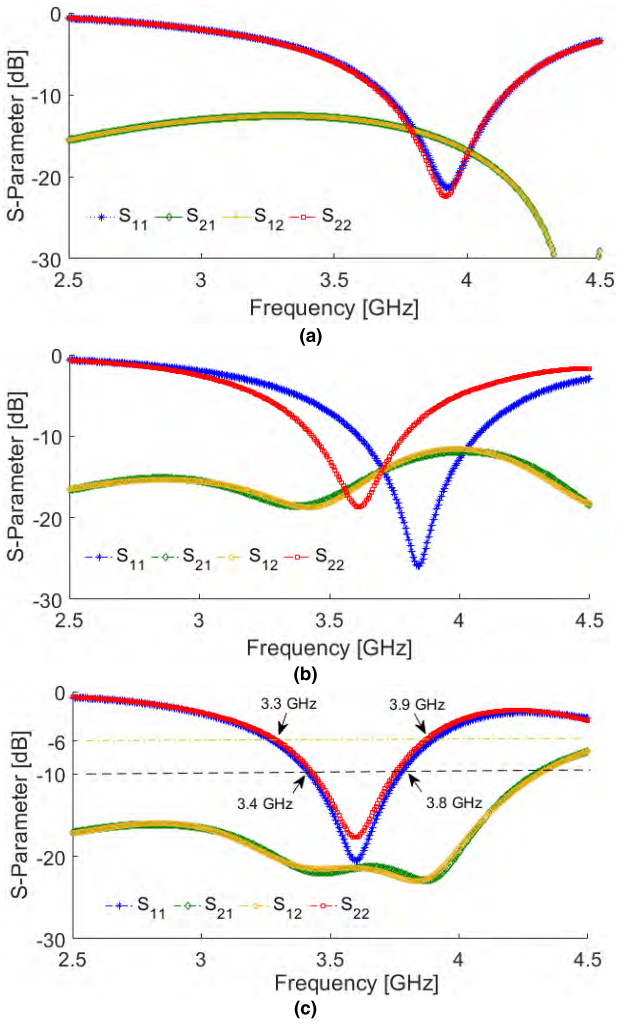

FIGURE 3. S-parameter results for the various designs illustrated in Fig. 2, respectively.

of 3.4-3.8 GHz is obtained for the antenna with different ports and polarizations. In addition, as can be found, the mutual coupling characteristic between the feeding ports of the dual-polarized square-ring slot antenna has been reduced significantly (from −13 dB to −23 dB).

The antenna performance for different positions of the embedded parasitic structures across the square-ring resonator (Fig. 4) has been studied in Fig. 5. As illustrated, the antenna frequency response and also the mutual coupling

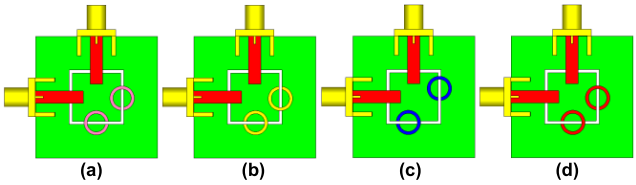

FIGURE 4. Different placement of the circular-ring/open-ended parasitic structures across the slot resonator.

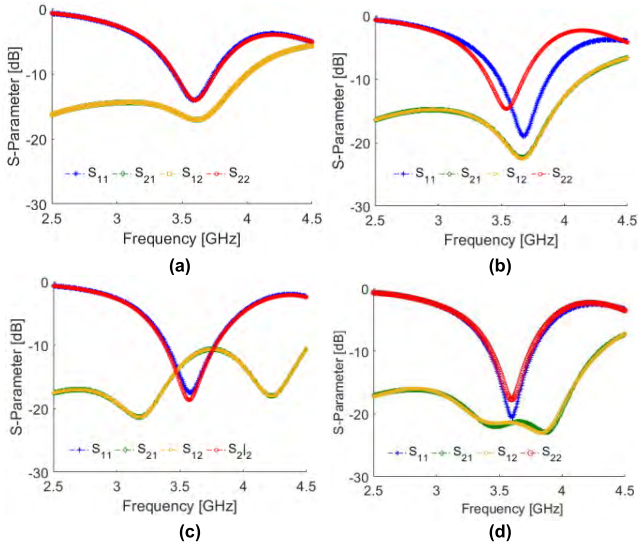

FIGURE 5. S-parameter results of the antenna for different positions of the parasitic structures shown in Fig. 4.

characteristics are highly depended on the location of the parasitic structures. Furthermore, as seen, the fourth configuration (Fig. 4 (d)) is the best choice and representing the highest coupling with similar S_{11}/S_{22} characteristics for the desired frequency range (3.4-3.8 GHz 5G band).

There are various design parameters of the proposed square-ring microstrip-fed slot antenna which have significant impacts on the antenna characteristics in terms of the operating band, the mutual coupling, and the impedance matching. The S_{11} characteristics of the antenna for various values of fundamental design parameters are studied in Fig. 6 and the obtained results have been discussed in the following.

One fundamental parameter relates to the length of the feed-lines (L_f). As seen in Fig. 6 (a), the feed-line length (L_f) impacts the impedance matching characteristic and for the values from 8.75 to 10.25 mm, the impedance matching function of the antenna reflection coefficient (S_{11}) can be tuned from less than −5 dB to more than −40 dB. The simulated S_{11} curves for different sizes of the slot-ring (W) are shown in Figure 6 (b): when its size decreases from 12.4 mm to 10.4 mm, the center of the operation frequency varies from 4.8 to 3.2 GHz while maintaining good impedance matching characteristic.

Another important parameter which tunes the operation frequency is the width of the ring slot (S_1). As illustrated

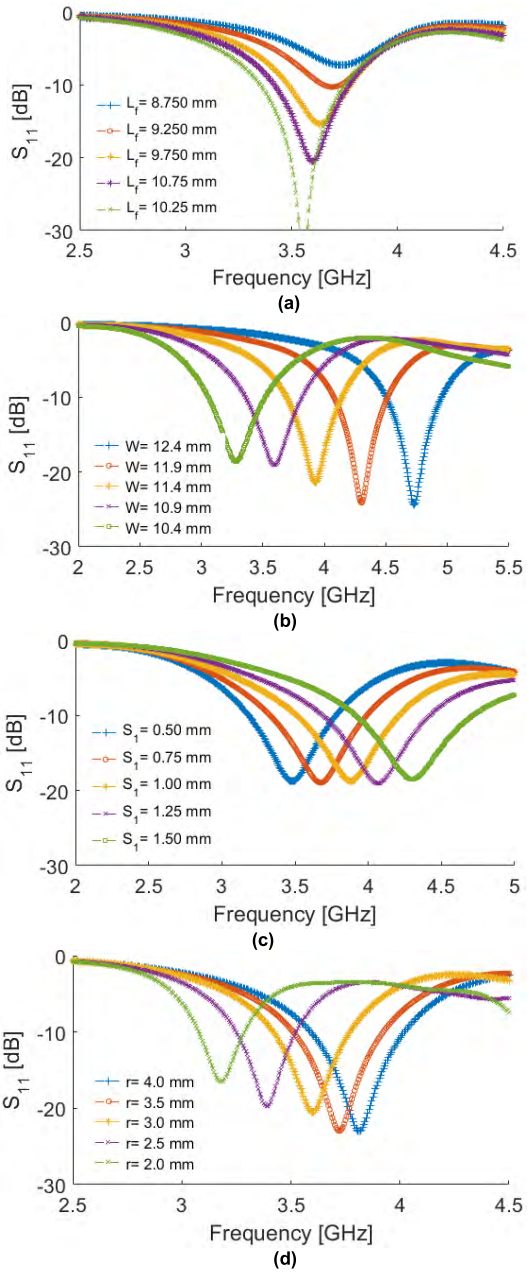

FIGURE 6. Antenna S_{11} results for different values of (a) L_f, (b) W, (c) S_1, and (d) r.

in Fig. 6 (c), the antenna response can be also easily tuned by changing the width of the square-ring slot. As mentioned above, the circular-ring/open-ended parasitic structures are embedded on the top layer and across the square-ring slot radiators and as shown in Fig. 6 (d), their radius (r) can affect not only the operation frequency but also the bandwidth of the proposed design.

Figure 7 illustrates the current distributions of the dual-polarized ring slot antenna at the resonance frequency (3.6 GHz) in the top and bottom layers. As depicted in Figs. 7(a) and 7(b), most of the currents have been distributed around the square-ring slot radiator in the ground plane. It can be seen for the different feeding ports, the

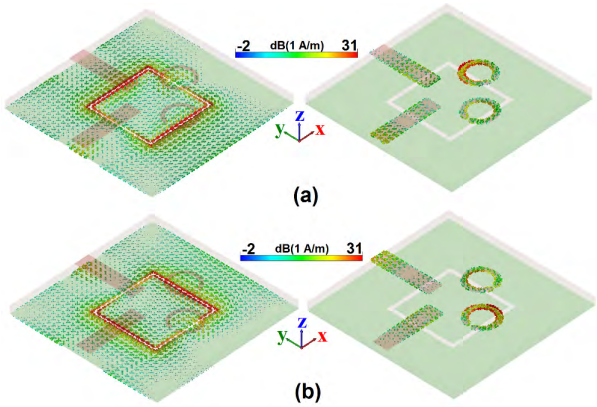

FIGURE 7. Current distribution at 3.6 GHz for (a) port 1 and (b) port 2.

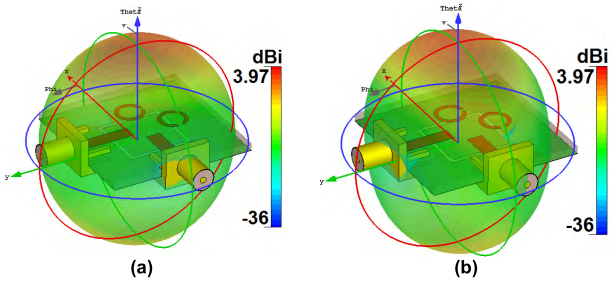

FIGURE 8. 3D transparent schematic of the antenna radiation patterns at 3.6 GHz for (a) port 1 and (b) port 2.

currents flow contrary to each other and provide the dual polarization characteristic [18]. In addition, as shown, the employed parasitic structures have high current densities and appear very active at 3.6 GHz.

The 3D views of the antenna radiation patterns at 3.6 GHz for different ports are displayed in Fig. 8. As shown, same radiation performances with different polarizations and also 3.97 dBi directivity are obtained for the proposed slot antenna design. It can be seen that the designed slot antenna provides dumbbell-shaped radiation patterns suitable to cover the top and bottom side of the smartphone PCB which can increase the radiation coverage of the 5G MIMO antenna design. The maximum gain and efficiencies for the differently-fed square-ring slot antenna are represented in Fig. 9. As seen, the antenna provides high efficiencies even though it is designed on the FR-4 dielectric. In addition, as can be observed, the antenna exhibits around 3 dBi maximum gain.

As illustrated in Fig. 10, a prototype of the single-element dual-polarized slot antenna was fabricated and its fundamental characteristics were tested in the Antenna Laboratory at the University of Bradford. Figures 11 (a) and (b) show the measurement setups used for the antenna S-parameter and radiation characteristics, respectively. As can be seen, the S-parameters of the antenna including S_{11}/S_{22} and S_{21}/S_{12} characteristics were measured using the network analyzer and the antenna radiation pattern was measured in the anechoic chamber.

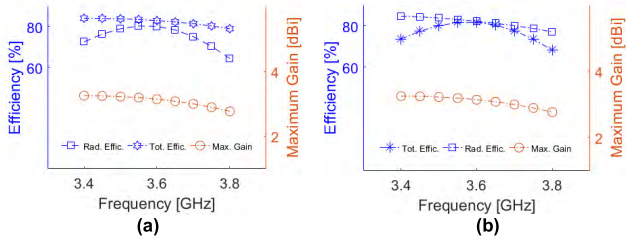

FIGURE 9. Efficiencies and maximum gains for (a) port 1 and (b) port 2.

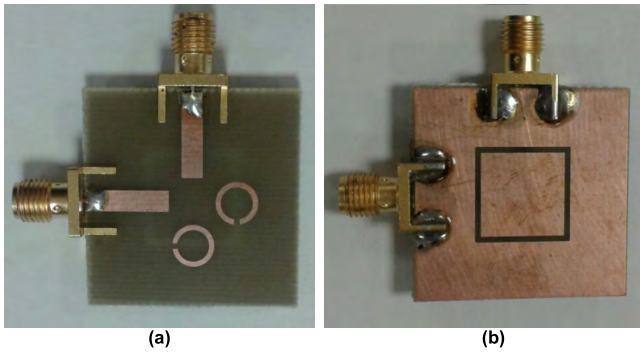

FIGURE 10. Fabricated antenna, (a) top view and (b) bottom view.

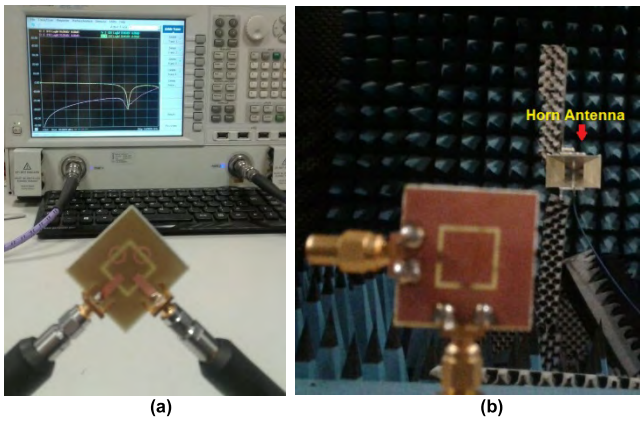

FIGURE 11. Measurement setups for (a) S-parameter and (b) radiation pattern of the fabricated antenna element.

The measured S-parameter results of the prototype are displayed in Fig. 12. As illustrated, the antenna provides very good impedance matching around 3.6 GHz (center frequency of the desired frequency band). High-isolation with more than −25 dB mutual coupling has been obtained for the fabricated sample. In addition, compared with the simulations (shown in Fig. 3 (c)), it can be confirmed that there is a good agreement between them. Figure 13 (a) shows the measured and simulated radiation patterns of the fabricated prototype at 3.6 GHz. As shown, the antenna exhibits a dumbbell-shaped radiation pattern with almost symmetrical schematic covering the top/bottom portions of the substrate. More than 3 dB IEEE gain with acceptable agreement has been achieved for the simulated and measured antenna radiation patterns. The simulation and measurement results of the antenna gain versus

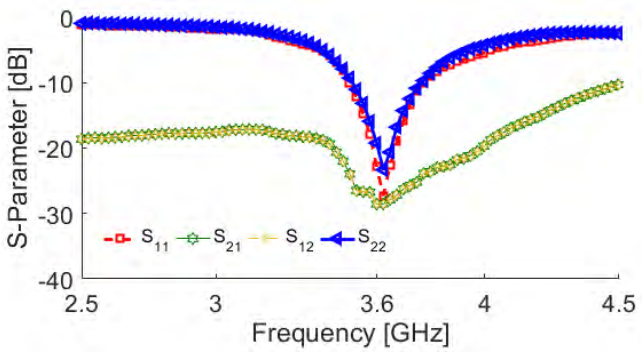

FIGURE 12. Measured S-parameters of the antenna element.

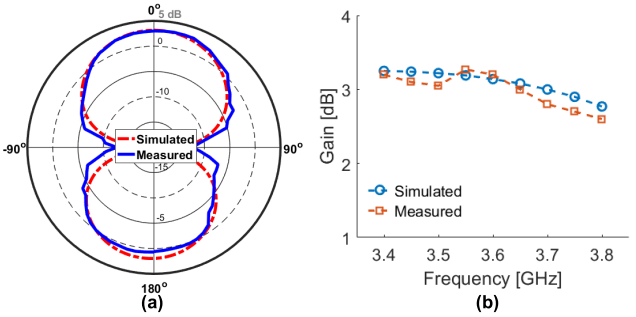

FIGURE 13. Measured and simulated (a) antenna radiation patterns and (b) its gain levels.

operation frequency are plotted in Fig. 13 (b). As shown, the antenna gain is almost constant and slightly varies around 3 dB.

III. THE PROPOSED MIMO 5G SMARTPHONE ANTENNA

Figure 14 displays the schematic of the proposed dual-polarized smartphone 5G antenna.

The proposed design is arranged on an FR4 dielectric with permittivity 4.4 and loss tangent 0.025 which has an overall dimension of 75 × 150 mm^2. The dual-polarized square-ring slot antenna elements with the reduced size of 25 × 25 mm^2 are placed at the corners of the smartphone PCB.

The simulated S-parameters including the reflection coefficient (S_{nn}) and the mutual coupling (S_{nm}) characteristics of the designed dual-polarized MIMO antenna array are shown in Fig. 15. Clearly, the radiation elements have similar return loss performances providing high impedance matching (around -20 dB reflection coefficients) at 3.6 GHz. Furthermore, as shown in Fig. 15 (b), the mutual coupling function of the antenna elements (less than −15 dB) are good enough to avoid the loss of radiation performance for the 5G smartphone antenna.

Employing the slot radiators on the proposed 5G array configuration not only exhibits sufficient bandwidth but also provides almost symmetrical radiation patterns to cover the top and bottom regions of the PCB. As shown in Fig. 16, the antenna elements can provide high directivity radiation patterns covering the top and bottom sides of PCB and improving the coverage efficiency function [19].

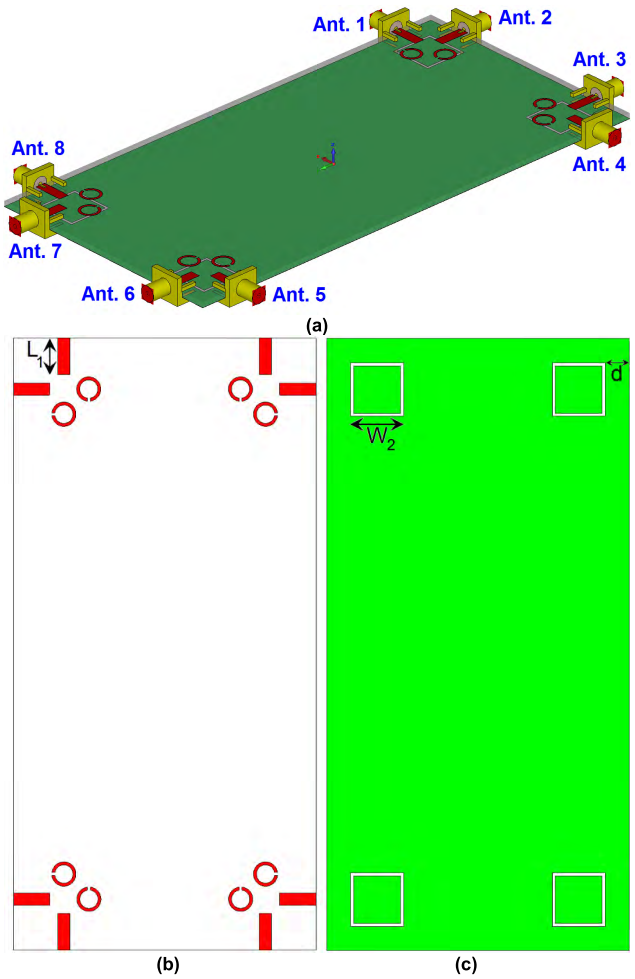

FIGURE 14. (a) 3D side view, (b) top and (b) bottom layers of the proposed 5G smartphone antenna.

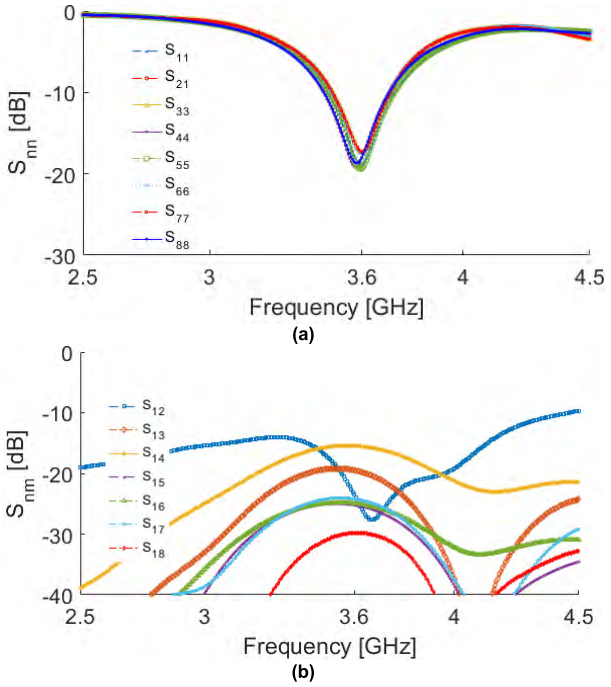

FIGURE 15. The antenna S-parameter results, (a) S_{nn} and (b) S_{nm}.

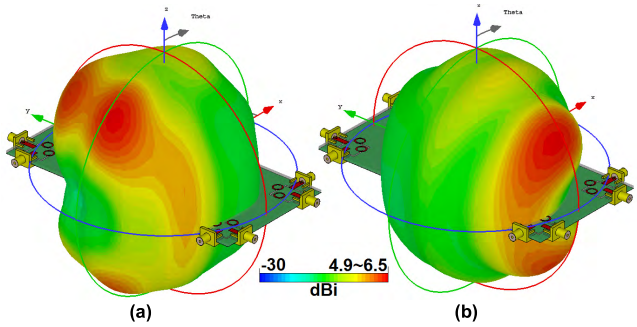

FIGURE 16. 3D radiation patterns (with directivity values) of a slot radiator with different feeding ports (a) port 1 and port (2).

Figure 17 displays the 3D top-views of the radiation patterns for each antenna elements deployed in the proposed 5G smartphone PCB. It can be seen, each side of the smartphone PCB can be covered by the radiation patterns of the radiators. At the same time, due to the dual-polarized characteristic of the antenna elements, different polarizations for each region of the PCB can be achieved which make the MIMO antenna system suitable for the future mobile terminal applications.

The radiation and total efficiencies of the dual-polarized antenna elements are illustrated in Fig. 18. As illustrated, the antenna elements have high radiation efficiencies. They also provide more than 70% total efficiencies at the resonance frequency (3.6 GHz). Furthermore, for the frequency range from 3.4 to 3.8 GHz (5G operation band), more than 75% radiation efficiency and 60% total efficiency characteristics have been achieved for the radiators of the proposed MIMO smartphone antenna.

The proposed smartphone 5G antenna design was properly fabricated on an FR-4 substrate and its properties in terms of radiation patterns and S-parameters were measured. Figures 19 (a) and 19 (b) illustrate the top and bottom views of the fabricated MIMO antenna system. In order to measure the system characteristics and also to avoid the mutual effect from the adjacent elements, 50-Ohm RF loads have been used for the antenna elements which are not under test. Figure 19 (c) shows the schematic of the MIMO system platform for measurement.

As shown, a pair of the antennas has been connected to the Network Analyzer cables to be tested. The measured S-parameters (S_{nn}/S_{nm}) of the MIMO antenna system are illustrated in Fig. 20. As can be observed, each single element of the MIMO design has sufficient S-parameter characteristics and in compared with the simulated results, the agreement is acceptable.

As can be seen from the 3D radiation patterns in Fig. 18, the slot antenna elements with the same polarizations provide almost the same performances. Due to this point, 2D polar radiation patterns of the adjacent microstrip-fed slot antennas with different polarizations have been measured. Figure 21 illustrates the simulation and measurement results

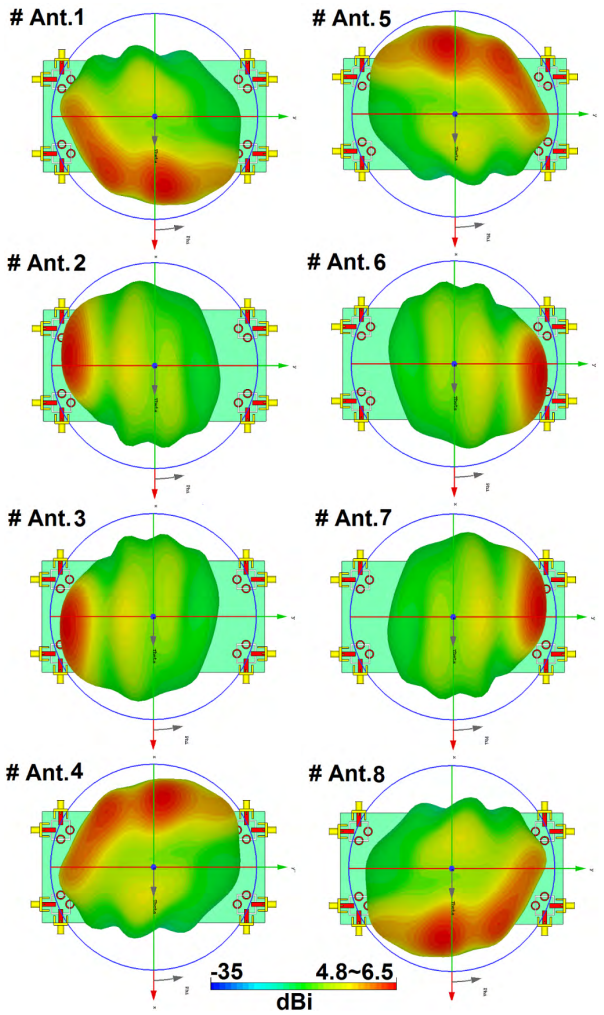

FIGURE 17. Radiation patterns for the antenna elements with directivity values at 3.6 GHz.

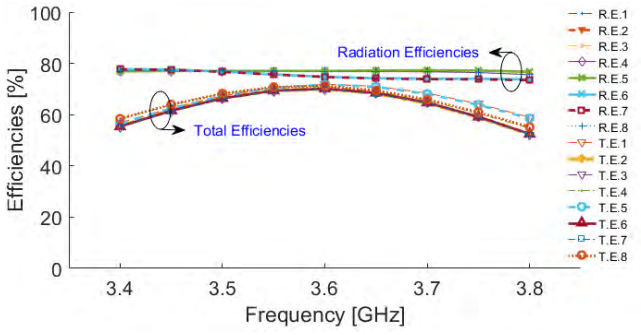

FIGURE 18. Efficiencies of the antenna elements.

of the antenna radiation patterns at 3.6 GHz. As can be seen, the fabricated prototype provides good radiation patterns similar to the simulated results. Furthermore, as seen, around 5 dB gain is obtained for the square-ring slot element with different polarizations.

The envelope correlation coefficient (ECC) of diverse antenna pairs is a typical function to judge multiple port

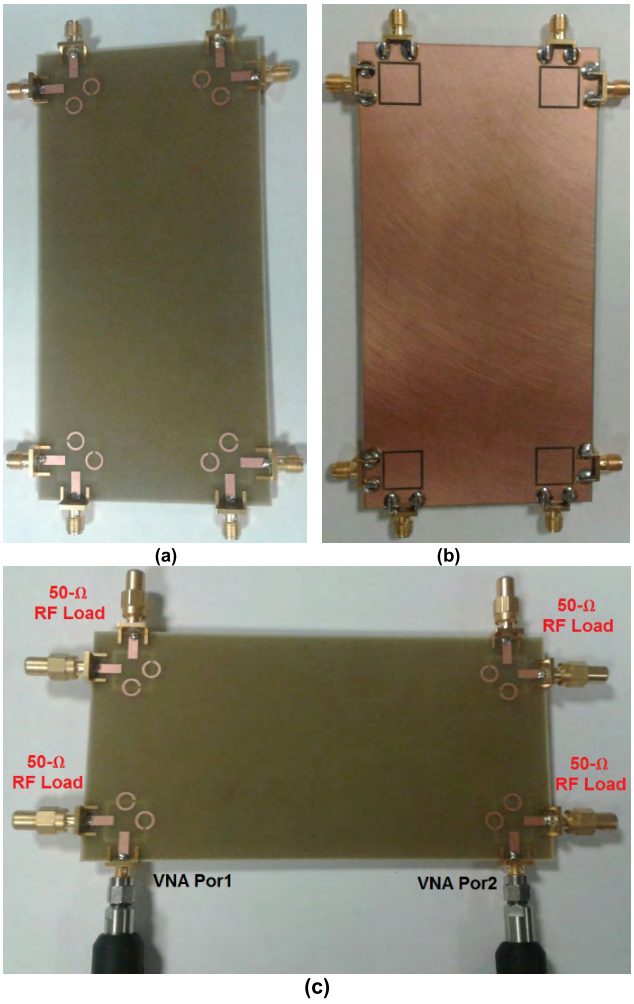

FIGURE 19. Fabricated smartphone antenna PCB, (a) top view, (b) bottom view, and (c) the prototype connected to the cables and loads.

performance of the MIMO antenna. The correlation among the embranchment signals received by different antennas is evaluated by this parameter, and lower ECC means more diversified patterns as a rule [20]. An acceptable standard for a desirable MIMO system is ECC < 0.5. Total active reflection coefficient (TARC) is another important parameter which must be also considered in MIMO antennas. The calculated ECC and TARC results of the proposed MIMO design form the simulations and measurements are presented in Fig. 22. The obtained results indicate that the calculated ECC function of the MIMO antenna elements is very low over the entire operating band. In addition, the results from the calculated TARC show that the higher mutual coupling can result in the higher TARC.

IV. USER-IMPACT AND SAR INVESTIGATION

Due to the importance of the user-impact on the radiation properties of a smartphone antenna system and also the specific absorption rate (SAR) effects of the smartphone antenna on the human head [21], the investigation on these parameters have been studied in this section. Figure 23 investigates the

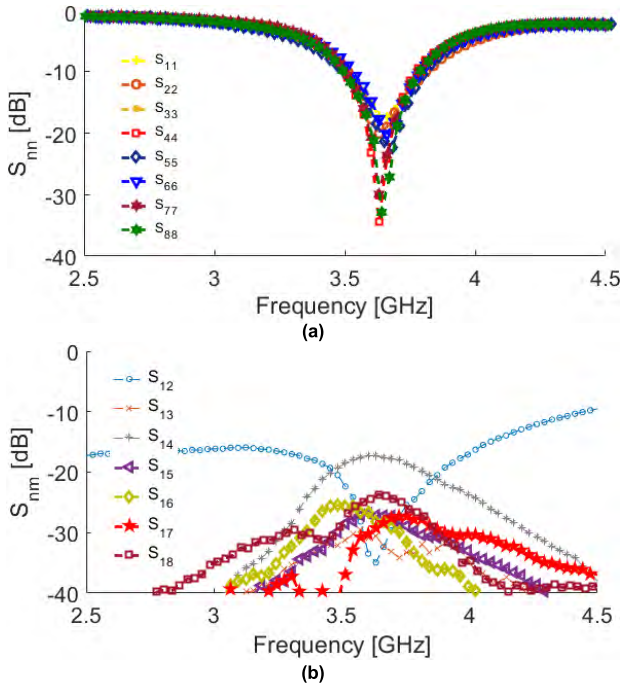

FIGURE 20. Measured S-parameter results of the proposed smartphone MIMO antenna, (a) S_{nn} and (b) S_{nm}.

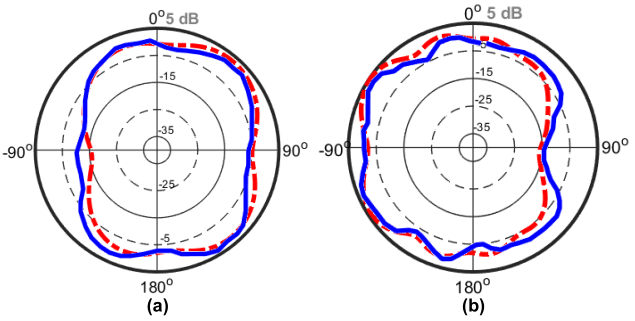

FIGURE 21. Measured (solid-lines) and simulated (dashed-line) 2D-polar radiation patterns of (a) antenna 1 and (b) antenna 2.

performance of the proposed MIMO smartphone antenna in terms of the total efficiency characteristic under right-hand mode (RHM) and left-hand mode (LHM) scenarios.

According to the simulations, the antenna elements show good performances in the vicinity of the user-hand and provide sufficient total efficiencies. The maximum reductions in total efficiently characteristic have been occurred for the antenna elements partially covered by hand tissue, especially Antennas 5 and 6 in RHM and Antennas 7 and 8 in LHM. It should be emphasized that this behavior is mainly because of hand tissue properties that is very lossy and can absorb the radiated power of the antenna. However, they still provide at least 20% total efficiency in 3.6 GHz and can still work in MIMO cellular communications. In addition, compared with the simulated total efficiencies, the performances of the antennas close to the finger have been reduced more than the elements far from the user's hand and fingers.

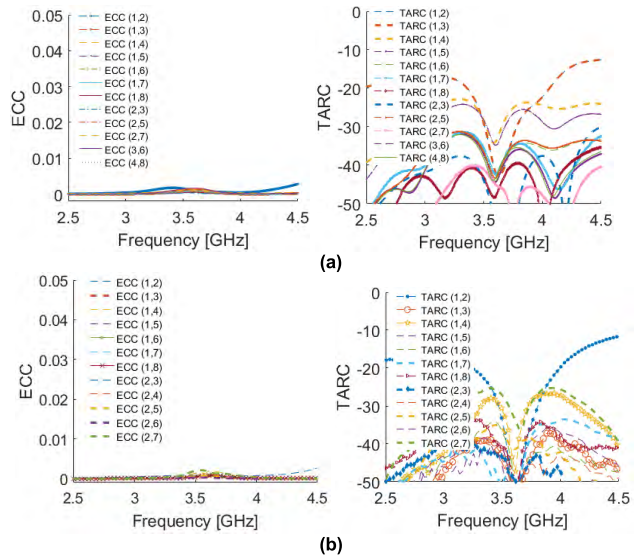

FIGURE 22. (a) Simulated and (b) Measured ECC and TARC results.

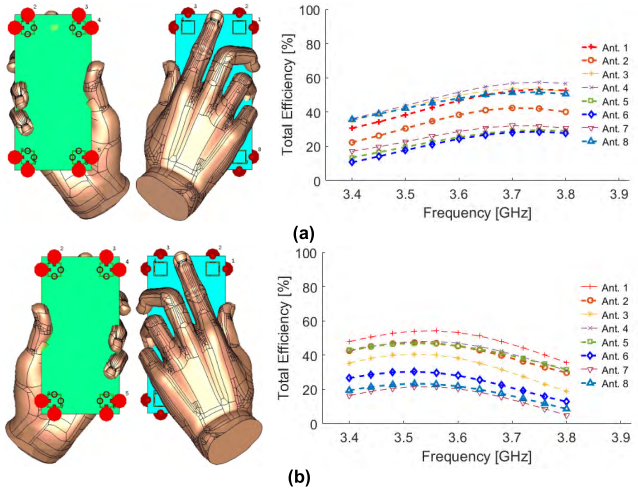

FIGURE 23. (a) Right Hand and (b) Left hand modes with the simulated efficiency results.

Figure 24 illustrates the radiation patterns of the antenna elements in the vicinity of the user's double-hands (read mode). As illustrated, the antenna elements provide good radiation patterns with sufficient gain values and pattern coverage. Clearly, the user's hand reduced the characteristics of the antenna, however, it is not very significant in this study. As seen, the antenna elements exhibit variable gain values with more than 1.9 dB.

SAR is the measurement function for the electromagnetic absorption of a human body during transmit and receive radio frequency data which is a critical issue for mobile terminal systems and should be as low as possible [22]. The simulated SAR values for the proposed design in the vicinity of the human-head at different frequencies are investigated in Fig. 25. As can be observed, the antenna has sufficient SAR values for the frequencies of 3.4, 3.6, and 3.8 GHz. The distance between MIMO antenna and the human-head in the

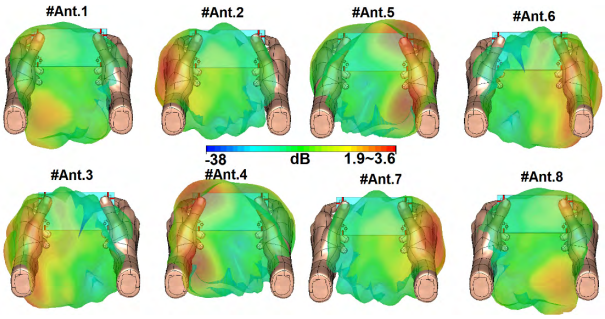

FIGURE 24. Radiation patterns of the different elements in Read-Mode.

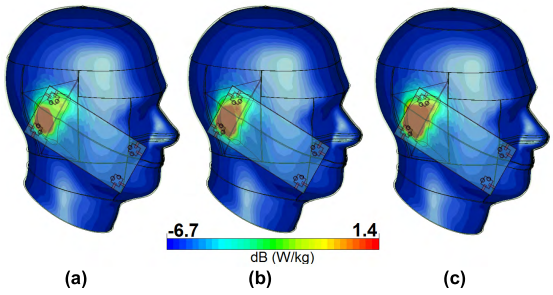

FIGURE 25. SAR investigation of the proposed MIMO antenna at, (a) 3.4 GHz, (b) 3.6 GHz, and (c) 3.8 GHz.

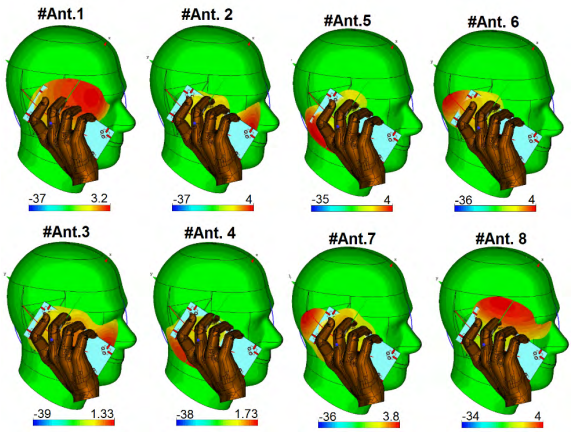

FIGURE 26. The radiation pattern of the antenna elements in Talk-Mode.

z-axis has a significant impact on the SAR values. It should be noted that the distance in this study is less than 10 mm.

Figure 26 depicts the radiation patterns for each antenna element of the proposed MIMO system in Talk-Mode (in the presence of user-hand/user-head). As seen, the proposed MIMO antenna system works well and provides sufficient gain values for each radiator used at different corners of the PCB. The obtained IEEE gain for the antenna elements varies from 1.3 to 4 dB and mainly depends on the locations of the antenna elements in the Talk-Mode scenario.

V. CONCLUSION

In this manuscript, a new design of reduced-coupling slot antenna array has been proposed for 5G MIMO mobile terminals. The structure of the proposed MIMO antenna was composed of dual-polarized square-ring slot antennas placed at the corners of the smartphone PCB. In order to reduce the mutual coupling of the antenna elements, a pair of circular-ring/open-ended parasitic structures was used on the top layer of the dielectric and across the square-ring slot radiator. Using the embedded parasitic structure, the mutual coupling of the adjacent radiators has been reduced significantly. The proposed MIMO antenna provides sufficient radiation coverage with dual-polarization at each side of the PCB. The MIMO antenna system was fabricated and tested and good agreements have been achieved between the simulation and measurements. Good radiation performances have been obtained for the MIMO antenna in the presence of user-head/user-hand. The proposed antenna offers sufficient characteristics for 3.6 GHz applications and might be a suitable candidate for use in 5G smartphone applications.

REFERENCES

[1] Q.-U.-A. Nadeem, A. Kammoun, M. Debbah, and M.-S. Alouini, "Design of 5G full dimension massive MIMO systems," *IEEE Trans. Commun.*, vol. 66, no. 2, pp. 726–740, Feb. 2018.

[2] A. Osseiran *et al.*, "Scenarios for 5G mobile and wireless communications: The vision of the METIS project," *IEEE Commun. Mag.*, vol. 52, no. 5, pp. 26–35, May 2014.

[3] *Statement: Improving Consumer Access to Mobile Services at 3.6 GHz to 3.8 GHz*. Accessed: Oct. 21, 2018. [Online]. Available: https://www.ofcom.org.uk/consultations-and-statements/category-1/future-use-at-3.6-3.8-ghz

[4] H. H. Yang and Y. Q. S. Quel, "Massive MIMO meet small cell," in *SpringerBriefs in Electrical and Computer Engineering*. Cham, Switzerland: Springer, 2017. doi: 10.1007/978-3-319-43715-6_2.

[5] Z. Qin, G.-Y. Wen, M. Zhang, and J. Wang, "Printed eight-element MIMO system for compact and thin 5G mobile handest," *Electron. Lett.*, vol. 52, no. 6, pp. 416–418, Mar. 2016.

[6] Y. Li, H. Zou, M. Wang, M. Peng, and G. Yang, "Eight-element MIMO antenna array for 5G/Sub-6GHz indoor micro wireless access points," in *Proc. Int. Workshop Antenna Technol. (iWAT)*, Nanjing, China, Mar. 2018, pp. 1–4.

[7] R. Hussain, A. T. Alreshaid, S. K. Podilchak, and M. S. Sharawi, "Compact 4G MIMO antenna integrated with a 5G array for current and future mobile handsets," *IET Microw., Antennas Propag.*, vol. 11, no. 2, pp. 271–279, 2017.

[8] A. A. Al-Hadi, J. Ilvonen, R. Valkonen, and V. Viikari, "Eight-element antenna array for diversity and MIMO mobile terminal in LTE 3500 MHz band," *Microw. Opt. Technol. Lett.*, vol. 56, no. 6, pp. 1323–1327, 2014.

[9] K.-L. Wong, J.-Y. Lu, L.-Y. Chen, W.-Y. Li, Y.-L. Ban, and C. Li, "16-antenna array in the smartphone for the 3.5-GHz MIMO operation," in *Proc. Asia–Pacific Microw. Conf.*, Nanjing, China, Dec. 2015, pp. 1–3.

[10] L. Sun, H. Feng, Y. Li, and Z. Zhang, "Compact 5G MIMO mobile phone antennas with tightly arranged orthogonal-mode pairs," *IEEE Trans. Antennas Propag.*, vol. 66, no. 11, pp. 6364–6369, Nov. 2018, doi: 10.1109/TAP.2018.2864674.

[11] Y. Li, C.-Y.-D. Sim, Y. Luo, and G. Yang, "Multiband 10-antenna array for sub-6 GHz MIMO applications in 5-G smartphones," *IEEE Access*, vol. 6, pp. 28041–28053, 2018.

[12] K.-L. Wong, C.-Y. Tsai, and J.-Y. Lu, "Two asymmetrically mirrored gap-coupled loop antennas as a compact building block for eight-antenna MIMO array in the future smartphone," *IEEE Trans. Antennas Propag.*, vol. 65, no. 4, pp. 1765–1778, Apr. 2017.

[13] M.-Y. Li, Z.-Q. Xu, Y.-L. Ban, C.-Y.-D. Sim, and Z.-F. Yu, "Eight-port orthogonally dual-polarised MIMO antennas using loop structures for 5G smartphone," *IET Microw., Antennas Propag.*, vol. 11, no. 12, pp. 1810–1816, 2017.

[14] M.-Y. Li *et al.*, "Eight-port orthogonally dual-polarized antenna array for 5G smartphone applications," *IEEE Trans. Antennas Propag.*, vol. 64, no. 9, pp. 3820–3830, Sep. 2016.

[15] Y. Liu, H. Yi, F.-W. Wang, and S.-X. Gong, "A novel miniaturized broadband dual-polarized dipole antenna for base station," *IEEE Antennas Wireless Propag. Lett.*, vol. 12, pp. 1335–1338, 2013.

[16] Y. Yoshimura, "A microstripline slot antenna (short papers)," *IEEE Trans. Microw. Theory Techn.*, vol. MTT-20, no. 11, pp. 760–762, Nov. 1972.
[17] D. Pozar, "A reciprocity method of analysis for printed slot and slot-coupled microstrip antennas," *IEEE Trans. Antennas Propag.*, vol. AP-34, no. 12, pp. 1439–1446, Dec. 1986.
[18] Z. N. Chen and X. M. Qing, "Dual-band circularly polarized *S*-shaped slotted patch antenna with a small frequency-ratio," *IEEE Trans. Antennas Propag.*, vol. 58, no. 6, pp. 2112–2115, Jun. 2010.
[19] X. Qing, Z. N. Chen, and T. S. P. See, "A multi-band MIMO antenna with full coverage," in *Proc. EuCA*, 2011, pp. 2497–2500, 2011.
[20] M. S. Sharawi, "Printed multi-band MIMO antenna systems and their performance metrics [wireless corner]," *IEEE Antennas Propag. Mag.*, vol. 55, no. 5, pp. 218–232, Oct. 2013.
[21] J. Moustafa, N. J. McEwan, R. A. Abd-Alhameed, and P. S. Excell, "Low SAR phased antenna array for mobile handsets," *Appl. Comput. Electromagn. Soc. J.*, vol. 21, no. 3, pp. 196–205, 2006.
[22] M. Fallah, A. A. Heydari, A. R. Mallahzadeh, and F. H. Kashani, "Design and SAR reduction of the vest antenna using metamaterial for broadband applications," *Appl. Comput. Electromagn. Soc. J.*, vol. 26, pp. 141–155, Feb. 2011.

NASER OJAROUDI PARCHIN was born in Germi, Iran, in 1986. He is currently pursuing the Ph.D. degree with the University of Bradford, U.K., where he is also a Research Assistant. He has authored or co-authored many technical journal and conference papers with 23 h-index and 55 i10-index. His research interests include multi-band/UWB antennas, mm-wave phased array antennas, MIMO/diversity antennas, Fabry resonators, microwave filters, reconfigurable structures, and electromagnetic wave propagation. He is also a Reviewer in many journals, such as the IEEE Access, the IEEE AWPL, and the IET MAP.

YASIR ISMAEL ABDULRAHEEM AL-YASIR was born in Basra, Iraq. He is currently pursuing the Ph.D. degree with the Radio Frequency and Sensor Design Research Group, University of Bradford, U.K. He was appointed as a Lecturer at Southern Technical University, Basra, in 2015. In 2016 and 2017, he was an Electrical Engineer with the Basra Oil Training Institute, Ministry of Oil, Iraq. He has co-authored two book chapters and has published many journals and conference papers on the aspects of wireless communications. His main interests include antennas, RF, and microwave circuit designs.

AMMAR H. ALI received the B.Eng. degree in electronic and communication engineering from the University of Technology, Baghdad, Iraq, in 2001, and the M.Sc. degree in communication network planning and management from the University of Portsmouth, U.K., in 2009. He is currently pursuing the Ph.D. degree with the Antennas and Applied Electromagnetics Research Group, Electronics, Communications and Information Systems Engineering Research Group, University of Bradford. He was with several telecommunication companies, which gave him practical experience beside his theoretical knowledge in telecommunication field. His research interest includes beam steering antenna design.

ISSA ELFERGANI received the M.Sc. and Ph.D. degrees in electronic and electrical engineering from the University of Bradford, U.K., in 2008 and 2012, with a specialization in tunable antenna design for mobile handset and UWB applications. He is currently a Senior Researcher with the Instituto de Telecomunicações, Aveiro, Portugal, working with European research-funded projects, while serving as a Technical Manager for ENIAC ARTEMIS, from 2011 to 2014, EUREKA BENEFIC, from 2014 to 2017, CORTIF, from 2014 to 2017, GREEN-T, from 2011 to 2014, VALUE, in 2016, H2020-SECRET Innovative Training Network, from 2017 to 2020, and THINGS2DO, from 2014 to 2018. He has published over 90 academic journal and conference papers; in addition, he has authored two books editorial and nine book chapters. His expertise includes research in various antenna designs, such as MIMO, UWB, balanced, and unbalanced antennas with the application of theoretical, computational analytical approaches, RF MEMS filter technologies, and power amplifier designs. He is a member of the IEEE and the American Association for Science and Technology.

JAMES M. NORAS is currently a Senior Lecturer with the School of Engineering, Design and Technology, University of Bradford, U.K. He is also the Director of five internationally franchised B.Eng. and M.Sc. courses in electrical and electronic engineering, has successfully supervised 18 Ph.D. students, and is currently supervising the research of 3 Ph.D. students. He has published 50 journal papers and 85 conference papers, in fundamental semiconductor physics, analog and digital circuit design, digital signal processing, and RF system design and evaluation. His main research interests include digital system design and implementation, DSP and coding for communication systems, and localization algorithms for mobile systems. He is a member of the Institute of Physics and a Chartered Physicist.

JONATHAN RODRIGUEZ received the master's degree in electronic and electrical engineering and the Ph.D. degree from the University of Surrey, U.K., in 1998 and 2004, respectively. In 2005, he became a Researcher with the Instituto de Telecomunicações, Portugal, where he was a member of the Wireless Communications Scientific Area. In 2008, he became a Senior Researcher, where he established the 4TELL Research Group targeting next-generation mobile systems. He has served as a Project Coordinator for major international research projects, including Eureka LOOP and FP7 C2POWER, while serving as a Technical Manager for FP7 COGEU and FP7 SALUS. He is currently the Coordinator of the H2020-SECRET Innovative Training Network. Since 2009, he has been an Invited Assistant Professor with the University of Aveiro, Portugal, and attained an Associate Level, in 2015. In 2017, he was appointed as a Professor of mobile communications with the University of South Wales, U.K. He has authored more than 400 scientific works, including ten book editorials. He is a Senior Member of the IEEE and has been a Chartered Engineer, since 2013, and has been a Fellow of the IET, since 2015.

RAED A. ABD-ALHAMEED (M'02–SM'13) received the B.Sc. and M.Sc. degrees from Basrah University, Basrah, Iraq, in 1982 and 1985, respectively, and the Ph.D. degree from the University of Bradford, West Yorkshire, U.K., in 1997, all in electrical engineering, where he is currently a Professor of electromagnetic and radio-frequency engineering. He has been a Research Visitor with Wrexham University, U.K., since 2009, covering the wireless and communications research areas. He is the Leader of Radio Frequency, Propagation, Sensor Design and Signal Processing Research Group; in addition to leading the Communications Research Group for years within the School of Engineering and Informatics, Bradford University. He has long years' research experience in the areas of radio frequency, signal processing, propagations, antennas, and electromagnetic computational techniques, and has published over 500 academic journal and conference papers; in addition, he has co-authored four books and several book chapters. His interests include 5G green communications systems, computational methods and optimizations, wireless and mobile communications, sensor design, EMC, MIMO systems, beam steering antennas, energy-efficient PAs, and RF predistorter design applications. He is the Fellow of the Institution of Engineering and Technology, a Fellow of the Higher Education Academy, and a Chartered Engineer. He is a Principal Investigator for several funded applications to EPSRCs and a Leader of several successful knowledge transfer programs, such as with Arris (previously known as Pace plc), Yorkshire Water plc, Harvard Engineering plc, IETG Ltd., Seven Technologies Group, Emkay Ltd., and Two World Ltd. He has also been a Co-Investigator in several funded research projects, including H2020 MARIE Skłodowska-CURIE ACTIONS: Innovative Training Networks "Secure Network Coding for Next Generation Mobile Small Cells 5G-US," Non-linear and demodulation mechanisms in biological tissue (Department of Health, Mobile Telecommunications and Health Research Programme), and Assessment of the Potential Direct Effects of Cellular Phones on the Nervous System (EU: collaboration with six other major research organizations across Europe). He received the Business Innovation Award for his successful KTP with Pace and Datong companies on the design and implementation of MIMO sensor systems and antenna array design for service localizations. He is the Chair of several successful workshops on Energy Efficient and Reconfigurable Transceivers: Approach Towards Energy Conservation and CO2 Reduction that addresses the biggest challenges for the future wireless systems. He was appointed as a Guest Editor of the *IET Science, Measurements and Technology* Journal, from 2009 to 2012.